Vehicle Yaw Control via Second Order Sliding Mode Technique

***Abstract*—The problem of vehicle yaw control is addressed in this paper, using an active differential and yaw rate feedback. A reference generator, designed to improve vehicle handling, provides the desired yaw rate value to be achieved by the closed loop controller. The latter is designed using second order sliding mode methodology to guarantee robust stability in front of disturbances and model uncertainties, which are typical of the automotive context. A feedforward control contribution is also employed to enhance the transient system response. The control derivative is constructed as a discontinuous signal, attaining a second order sliding mode on a suitably selected sliding manifold. Thus, the actual control input results in being continuous, as it is needed in the considered context. Simulations performed using a realistic nonlinear model of the considered vehicle show the effectiveness of the proposed approach.**

***Index Terms*—Higher order sliding modes, robust control, chattering avoidance, vehicle yaw control.**

I. Introduction

Vehicle active stability systems aim to improve safety during emergency maneuvers and in critical driving conditions [1]. The employed actuators modify the vehicle dynamics by applying differential distribution of braking/driving forces or front and rear steering angles in a suitable way (see e.g. [2]–[6]). Additionally, stability systems that do not rely on braking forces can be employed in normal driving situations, in order to improve the vehicle manoeuvrability. However, any stability system has a limited capability of generating the control action, due to actuator and tyre limits. This could deteriorate the control performances or cause vehicle instability. Moreover, since the vehicle operates under a wide range of conditions of speed, load, road friction, etc., the active control system has to guarantee safety (i.e. stability) performances robustly in face of disturbances and model uncertainties. Robustness of active vehicle systems is a widely studied topic and significant results have been proposed (see e.g. [3]–[8]). In this paper, the problem of yaw control is addressed considering a vehicle equipped with a Rear Active Differential (RAD) [9]–[14]. A yaw rate feedback is employed in the proposed control structure, composed by a reference generator designed to improve vehicle handling, a closed loop controller, and a feedforward contribution. The feedback controller has to guarantee robust stability as well as good damping and readiness properties, while the feedforward contribution is used to further enhance the system performance in the transient phase.

The robust control technique used to design the feedback controller proposed in this paper is the so–called second order sliding mode control [15]–[18]. Second order sliding mode control can be viewed as the development of conventional (i.e., first order) sliding mode [19], [20]. Conventional sliding mode already guarantees the robustness features suitable to deal with the uncertainty sources and disturbances typical of automotive applications. Yet, conventional sliding mode control laws produce discontinuous control inputs [19], [20] which can generate high frequency chattering, with the consequent excessive mechanical wear and passengers' discomfort.

In contrast, second order sliding mode controllers generate continuous control actions, since the discontinuity necessary to enforce a sliding mode is confined to the derivative of the control signal, while the control signal itself is continuous. Apart from the robustness features against possible disturbances and parameter variations affecting the vehicle model, the sliding mode control methodology has the advantage of producing low complexity control laws compared to other robust control approaches (see e.g. [4]–[6], [11]) which appears particularly suitable to be implemented in the Electronic Control Unit (ECU) of a controlled vehicle. The second order sliding mode control scheme proposed in this paper provides performances similar to that obtained with the IMC controller presented in [5], with the advantage of producing less aggressive control variable behavior during transients, as shown in [12], [13]. Moreover, the proposed control scheme enables to take into account the saturation of the RAD actuator in a simpler way than that adopted in [5].

To test in a realistic way the effectiveness of the proposed control approach, simulations are performed using a detailed nonlinear 14 degrees of freedom vehicle model, which proves to give a good description of the vehicle dynamics as compared with real data. The paper is organized as follows. In Section II the problem formulation and the control objectives are indicated, while the vehicle model is presented in Section III. The proposed control scheme is described in Section IV, together with the related design techniques. Section V deals with simulation results. Finally, conclusions are drawn in Section VI.

II. Problem formulation and control requirements

The first control objective of any active stability system is to improve safety in critical maneuvers and in presence of unusual external conditions, such as strong lateral wind or changing road friction coefficient. Moreover, the considered RAD device can be employed to change the steady state and dynamic behaviour of the car, improving its handling properties. The vehicle inputs are the steering angle δ, commanded by the driver, and the external forces and moments applied to the vehicle centre of gravity. The most significant variables describing the behaviour of the vehicle are its speed $v(t)$, lateral acceleration $a_y(t)$, yaw rate $\dot{\psi}(t)$ and side slip angle $\beta(t)$. Regarding the vehicle as a rigid body moving at constant speed v, the following relationship between $a_y(t)$, $\dot{\psi}(t)$ and

$\dot{\beta}(t)$ holds

$$a_y(t) = v(\dot{\psi}(t) + \dot{\beta}(t)) \tag{1}$$

In steady state motion $\dot{\beta}(t) = 0$, thus lateral acceleration is proportional to yaw rate through the vehicle speed. In this situation, let us consider the uncontrolled car behaviour: for each constant speed value, by means of standard steering pad maneuvers it is possible to obtain the steady state lateral acceleration a_y corresponding to different values of the steering angle δ. These values can be graphically represented on the so–called *steering diagram* (see Fig. 1, dotted line). Such curves are mostly influenced by road friction and depend on the tyre lateral force–slip characteristics. At low acceleration the shape of the steering diagram is linear and its slope is a measure of the readiness of the car: the lower this value, the higher the lateral acceleration reached by the vehicle with the same steering angle, the better the maneuverability and handling quality perceived by the driver [21]. At high lateral acceleration the behaviour becomes nonlinear showing a saturation value, that is the highest lateral acceleration the vehicle can reach. The intervention of an active differential device can be considered as a yaw moment $M_z(t)$ acting on the car centre of gravity: such a moment is capable of changing, under the same steering conditions, the behaviour of a_y, modifying the steering diagram according to some desired requirements. Thus, a target steering diagram (as shown in Fig. 1, solid line) can be introduced to take into account the performance improvements to be obtained by the control system. More details about the generation of such target steering diagrams are reported in Section IV-A. Therefore, the

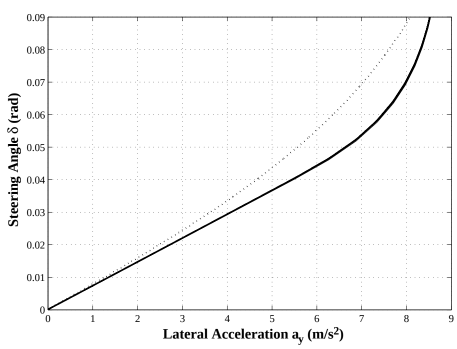

Fig. 1. Uncontrolled vehicle (dotted), and target (solid) steering diagrams. Vehicle speed: 100 km/h

choice of yaw rate $\dot{\psi}$ as the controlled variable is fully justified, also considering its reliability and ease of measurement on the car. A reference generator will provide the desired values $\dot{\psi}_{ref}$ for the yaw rate $\dot{\psi}$ needed to achieve the desired performances by means of a suitably designed feedback control law.

As for the generation of the required yaw moment $M_z(t)$, in this paper a full RAD is considered (see [9]–[14] for details). A schematic of the RAD taken into account in this paper is reported in Fig. 2. This device is basically a traditional bevel gear differential that has been modified in order to transfer motion to two clutch housings, which rotate together with the input gear. Clutch friction discs are fixed on each differential output axle. The ratio between the input angular speed of the

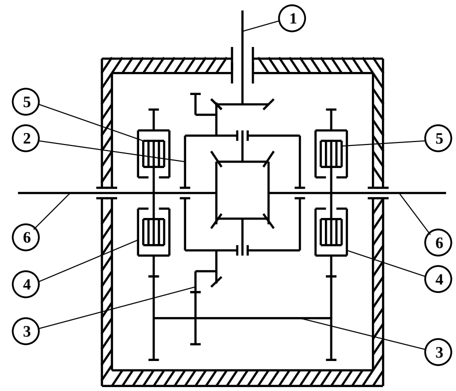

Fig. 2. Rear Active Differential schematic. The input shaft 1 transfers driving power to the traditional bevel gear differential 2 and, through the additional gearing 3, to the clutch housings 4. Clutch discs 5 are fixed to the output axles 6.

differential and the angular speeds of the clutch housings is such that the latter rotate faster than their respective discs in almost every vehicle motion condition (i.e. except for narrow cornering at very low vehicle speed), thus the sign of each clutch torque is always known and the torque magnitude only depends on the clutch actuation force, which is generated by an electro–hydraulic system whose input current is determined by the controller. The main advantage of this system is the capability of generating yaw moment of every value within the actuation system saturation limits, regardless of the input driving torque value and the speed values of the rear wheels. The considered device has a yaw moment saturation value of ± 2500 Nm, due to the physical limits of its electro–hydraulic system.

The actuator dynamics can be described by the following first order model [5]

$$G_A(s) = \frac{M_z(s)}{I_M(s)} = \frac{K_A}{1 + s/\omega_A} \tag{2}$$

where I_M is the input current originated by the controller and M_z is the actual yaw moment provided by RAD to the vehicle. The gain K_A depends on the geometry of the RAD, and ω_A is the bandwith of the electro–hydraulic valve.

The considered device has an input current limitation of ± 1 A which corresponds to the range of allowed yaw moment values (i.e. ± 2500 Nm) that can be mechanically generated.

As previously described, the improvements on the performances of the vehicle may be obtained using suitable modifications of the yaw dynamics in steady state conditions. Moreover, in critical maneuvering situations, such as fast path changing at high speed or braking and steering with low and non uniform road friction, the vehicle dynamics need to be improved in order to enhance stability and handling performances. Thus, the dynamic vehicle behaviour needs to satisfy good damping and readiness properties, which can be taken into account by a proper design of the feedback controller and the use of a feedforward action based on the driver input (i.e. δ) to increase system readiness. Indeed, the safety requirement (i.e. stability) needs to be guaranteed in face of the uncertainties arising from the wide range of the vehicle operating conditions of speed, load, tyre, friction, etc. Thus, a robust control design technique has to be used.

III. The Vehicle Model

In the present work, the control design is carried out relying on a single track linear model of the vehicle [1], [22], depicted in Fig. 3. This model is based on the assumption that the vehicle is travelling on a flat road with a low or zero longitudinal acceleration. Moreover, the wheel self–aligning moments are neglected and the longitudinal motion resistances are ignored compared to the tyre lateral forces. The relationship between the lateral force produced by a tyre and the sideslip angle is obtained by linearizing the so–called "Magic Formula" developed by Bakker and Pacejka [23] under the assumption of small sideslip angle. The dynamic generation mechanism of tyre forces is also modelled by introducing the tyre lateral relaxation lengths. The equations describing the motion of the

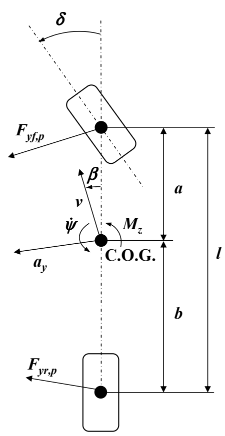

Fig. 3. The single track model.

vehicle are given by:

$$\begin{aligned} &mv(t)\dot\beta(t) + mv(t)\dot\psi(t) = F_{yf,p}(t) + F_{yr,p}(t)\\ &J_z\ddot\psi(t) = aF_{yf,p}(t) - bF_{yr,p}(t) + M_z(t)\\ &F_{yf,p}(t) + \tfrac{l_f}{v(t)}\dot F_{yf,p}(t) = -c_f(\beta(t) + \tfrac{a}{v(t)}\dot\psi(t) - \delta(t))\\ &F_{yr,p}(t) + \tfrac{l_r}{v(t)}\dot F_{yr,p}(t) = -c_r(\beta(t) - \tfrac{b}{v(t)}\dot\psi(t)) \end{aligned} \tag{3}$$

where m is the vehicle mass, J_z is the moment of inertia around the vertical axis, l is the wheel base, a and b are the distances between the centre of gravity and the front and rear axles respectively, l_f and l_r are the front and rear tyre relaxation lengths, c_f and c_r are the front and rear tyre cornering stiffnesses. $F_{yf,p}$ and $F_{yr,p}$ are the front and rear tyre lateral forces, δ is the front steering angle, β is the vehicle sideslip angle, ψ is the vehicle yaw angle and v is the vehicle speed. The control variable is the yaw moment M_z applied by the RAD.

IV. The Proposed Control Scheme

The proposed control structure is depicted in Fig. 4. The yaw rate reference signal $\dot\psi_{\text{ref}}(t)$ is generated by a nonlinear static map $\mathcal{M}$ which uses as inputs the front steering angle $\delta(t)$ and the vehicle speed $v(t)$. The feedback controller $\mathcal{C}$ is designed

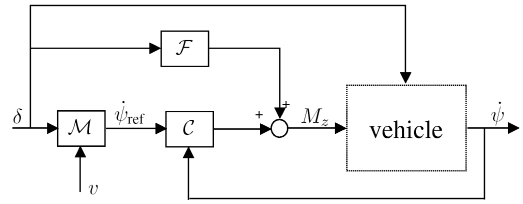

Fig. 4. Considered control structure.

relying on the second order sliding mode methodology (see [15], [16], [24]) and has the aim to determine the yaw moment contribution needed to track the required yaw rate performances described by $\dot\psi_{\text{ref}}(t)$. In order to improve the yaw rate transient behaviour exploiting the knowledge of the driver action, a feedforward contribution $\mathcal{F}$ produced on the basis of the driver input $\delta(t)$ has been added.

Hence, in order to implement the proposed control scheme on a real vehicle, the controlled vehicle must be equipped with sensors capable of measuring the yaw rate $\dot\psi$, the steering angle δ, and the wheels velocity, which is needed to estimate the vehicle speed v. All these sensors have low costs and are present in all the vehicles provided with a yaw control system.

A. Yaw Reference generator

As previously mentioned, the yaw rate reference is generated using a nonlinear static map, i.e., $\dot\psi_{\text{ref}}(t) = f(\delta(t), v(t))$ which uses as input the steering angle $\delta(t)$ and the vehicle speed $v(t)$. As in [5], a nonlinear steady state single track vehicle model is adopted to compute the map values. The model equations are the following

$$\begin{aligned} &m\,v\,\dot\psi = F_{yf,p}(\beta,\dot\psi,\delta,F_{zf}) + F_{yr,p}(\beta,\dot\psi,F_{zr})\\ &aF_{yf,p}(\beta,\dot\psi,\delta,F_{zf}) - bF_{yr,p}(\beta,\dot\psi,F_{zr}) + M_z = 0 \end{aligned} \tag{4}$$

where the front and rear tyre lateral forces $F_{yf,p}$ and $F_{yr,p}$ are computed considering the nonlinear tyre slip–lateral force relationship introduced in [23]. The nonlinear model (4) is employed to compute the uncontrolled vehicle steering diagram (i.e. $M_z = 0$) for each constant speed value within the working region of the vehicle (see Fig. 1, dotted line), as well as the reference steering diagram. The latter is calculated to improve the handling quality perceived by the driver [21]. In particular, the reference curves have been chosen to decrease the steering diagram slope in the linear tract (which is related to the vehicle understeer gradient [1]), thus improving the vehicle maneuverability in the linear zone, and to increase the maximum lateral acceleration that can be reached (as can be seen in Fig. 1, solid line). The nonlinear single track vehicle model (4) is also employed to verify that the designed reference steering diagrams correspond to feasible vehicle motion conditions, according to the actuator and tyre limits. The map of values of $\dot\psi_{\text{ref}}$ is obtained by designing a reference steering diagram for each value of velocity v within the working region of the vehicle. Fig. 5 shows an example of such a static reference map (see [5] for a more detailed description on the map construction).

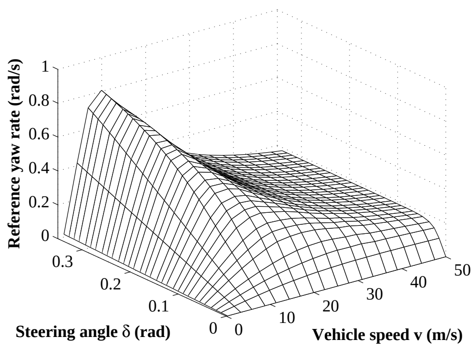

Fig. 5. An example of yaw rate reference static map.

B. The feedforward component design

As previously discussed, in order to improve the yaw rate transient response a further control input generated by a feedforward controller $\mathcal{F}$ driven by the steering angle $\delta(t)$ is added (see Fig. 4). In order to design the feedforward controller, the following transfer functions in the Laplace domain are obtained from the vehicle model equations (3)

$$\dot{\psi}(s) = G_\delta(s)\delta(s) + G_M(s)M_z(s) \tag{5}$$

where

$$\begin{aligned} G_\delta(s) &= \frac{b_2s^2 + b_1s + b_0}{a_4s^4 + a_3s^3 + a_2s^2 + a_1s + a_0} \\ G_M(s) &= \frac{c_3s^3 + c_2s^2 + c_1s + c_0}{a_4s^4 + a_3s^3 + a_2s^2 + a_1s + a_0} \end{aligned} \tag{6}$$

and

$$\begin{aligned} & a_4 = mJ_zl_fl_r,\ a_3 = mvJ_z(l_f + l_r) \\ & a_2 = J_z(mv^2 + c_fl_r + c_rl_f) + m(c_fa^2l_r + c_rb^2l_f) \\ & a_1 = v(J_z(c_f + c_r) + m(c_fa(a - l_r) + c_rb(b + l_f))) \\ & a_0 = c_fc_rl^2 - mv^2(c_fa + c_rb) \\ & b_2 = mvac_fl_r,\ b_1 = mv^2ac_f,\ b_0 = vc_fc_rl \\ & c_3 = ml_fl_r,\ c_2 = mv(l_f + l_r) \\ & c_1 = mv^2 + c_fl_r + c_rl_f,\ c_0 = v(c_f + c_r) \end{aligned} \tag{7}$$

The feedforward contribution is computed by means of a linear filter $F(s)$ to match the open loop yaw rate behaviour given by (5) with the one described by an objective transfer function $T_\delta^{\text{des}}(s)$, i.e.,

$$\dot{\psi}(s) = T_\delta^{\text{des}}(s)\delta(s) \tag{8}$$

Thus, considering the transfer function (5) where $M_z(s)$ is computed as $M_z(s) = F(s)\delta(s)$ and $\dot{\psi}(s)$ is given by (8), the feedforward filter $F(s)$ is obtained as

$$F(s) = \frac{T_\delta^{\text{des}}(s) - G_\delta(s)}{G_M(s)} \tag{9}$$

Since the feedforward controller aims to improve the transient response only, its contribution should be zero in steady state conditions. To satisfy this condition, $T_\delta^{des}(s)$ and $G_\delta(s)$ must have the same static gain.

C. Second order sliding mode control design

A second order sliding mode is a movement of a dynamic system confined to a particular subspace, named sliding manifold, which can be mathematically described in Filippovs' sense [25]. The second order sliding mode is determined by

$$S(x) = \dot{S}(x) = 0 \tag{10}$$

where $S(x)$, the so–called sliding variable, is a smooth function of the state x of the considered dynamical system, and $S(x) = 0$ identifies the sliding manifold. Second order sliding mode control generalizes the basic sliding mode control idea, acting on the second order time derivative of the system deviation from the sliding manifold, instead that on the first derivative, as it happens in first order sliding mode control design [20]. The main advantage of the second order sliding mode control introduced in [15] is that, in case of system with relative degree equal to one, it generates a continuous control action with a consequent reduction of the so–called chattering effect. Moreover, second order sliding mode control features a higher accuracy with respect to first order sliding mode control, while keeping the same robustness with respect to matched uncertainties [15], [16].

In the considered problem, the chosen sliding variable is the error between the actual yaw rate and the reference yaw rate, i.e.,

$$S(t) = \dot{\psi}(t) - \dot{\psi}_{ref}(t) \tag{11}$$

The control objective is to make this error vanish. By virtue of the use of sliding mode control it is possible to make the error converge to zero in finite time. To design the proposed controller, it is useful to observe that the first and second time derivative of the sliding variable are, respectively,

$$\dot{S}(t) = (aF_{yf,p}(t) - bF_{yr,p}(t) + M_z(t))/J_z - \ddot{\psi}_{ref}(t) \tag{12}$$

$$\ddot{S}(t) = (a\dot{F}_{yf,p}(t) - b\dot{F}_{yr,p}(t) + \dot{M}_z(t))/J_z - \dddot{\psi}_{ref}(t) \tag{13}$$

Introducing the auxiliary variables $y_1(t) = S(t)$ and $y_2(t) = \dot{S}(t)$, (12) and (13) can be rewritten as

$$\begin{cases} \dot{y}_1(t) = y_2(t) \\ \dot{y}_2(t) = \lambda(t) + \tau(t) \end{cases} \tag{14}$$

where $\tau(t) = M_z(t)/J_z$ is regarded as the auxiliary control variable and

$$\lambda(t) = (a\dot{F}_{yf,p}(t) - b\dot{F}_{yr,p}(t))/J_z - \dddot{\psi}_{ref}(t)$$

On the basis of physical consideration, the quantity $\lambda(t)$ can be assumed to be bounded with known bound, i.e,

$$|\lambda(t)| \leq \Lambda \tag{15}$$

where $\Lambda > 0$ depends on the operating condition of the vehicle. Note that a conservative estimation for Λ can be determined on the basis of (3), (4), and the tyre characteristic. Moreover, the quantity y_2 can be viewed as an unmeasurable quantity, being the first derivative of y_1 which depends on $\lambda(t)$ and $\tau(t)$.

Then, the control problem can be reformulated as follows: given system (14), where $\lambda(t)$ satisfies (15), and y_2 is unavailable for measurement, design the auxiliary control signal

$\tau(t)$ so as to steer y_1, y_2 to zero in finite time.
The second order sliding mode controller proposed in this paper is of sub–optimal type [24]. This implies that, under the assumption of being capable of detecting the extremal values $y_{1_{Max}}$ of the signal y_1, the following theorem can be proved:

Theorem 1: Given system (14), where $\lambda(t)$ satisfies (15), and y_2 is not measurable, the auxiliary control law

$$\tau(t) = \dot{M_z}(t)/J_z = -K_{SL}\ sign\Big\{y_1(t) - \frac{1}{2}y_{1M}(t)\Big\} \quad (16)$$

where the control gain K_{SL} is chosen such that

$$K_{SL} > 2\Lambda \quad (17)$$

and $y_{1M}(t)$ is a piece–wise constant function representing the value of the last singular point of $y_1(t)$ (i.e., the most recent value $y_{1M}(\bar{t})$ such that $\dot{y}_1(\bar{t}) = 0$), causes the convergence of the system trajectory to the origin of the plane, i.e., $y_1 = y_2 = 0$, in finite time.

Proof: The control law (16) is a sub–optimal second order sliding mode control law. So, by following a theoretical development as that provided in [24] for the general case, it can be proved that the trajectories on the y_1Oy_2 plane are confined within limit parabolic arcs including the origin. The absolute values of the coordinates of the trajectory intersections with the y_1, and y_2 axis decrease in time. As shown in [17], under condition (15) the following relationships hold

$$|y_1(t)| \le |y_{1M}(t)| \qquad |y_2(t)| \le \sqrt{|y_{1M}(t)|}$$

and the convergence of $y_{1M}(t)$ to zero takes place in finite time [17]. As a consequence, also $y_1(t)$ and $y_2(t)$ tend to zero in finite time since they are both bounded by $y_{1M}(t)$. ■
The saturation of the control input is taken into account relying on the approach proposed in [26]. We assume that the saturation value of the RAD is such that

$$M_{z,sat} > aF_{yf,p}(t) - bF_{yr,p}(t) - J_z\ddot{\psi}_{ref}(t) \quad (18)$$

Then, the actual control law $M_z(t)$ is given by

$$\dot{M_z}(t) = \begin{cases} -M_z(t) & \text{if } |M_z(t)| \ge M_{z,sat} \\ J_z\tau(t) & \text{otherwise} \end{cases} \quad (19)$$

where $\tau(t)$ is given by (16) and $M_{z,sat}$ is the saturation value of the RAD, i.e., 2500 Nm.
Note that assumption (18) implies that also a first order control law

$$M_z(t) = -M_{z,sat}\ sign\{S(t)\} \quad (20)$$

is capable of making $S(t) = 0$ in finite time. Yet, this is a discontinuous control law, which can produce the undesirable chattering effect.
As for the control design, the dynamic of the RAD actuator is neglected and the steady state gain of (2) is considered. Then the input current of the RAD is generated as

$$I_M(t) = M_z(t)/K_A \quad (21)$$

where $M_z(t)$ is obtained by integration of (19).

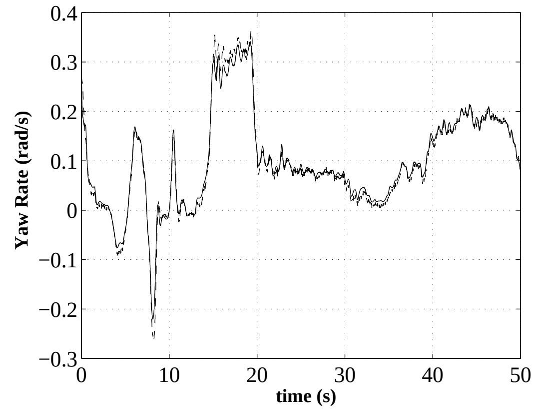

Fig. 6. Comparison between the yaw rate real data (dashed) and that obtained with the considered model (solid).

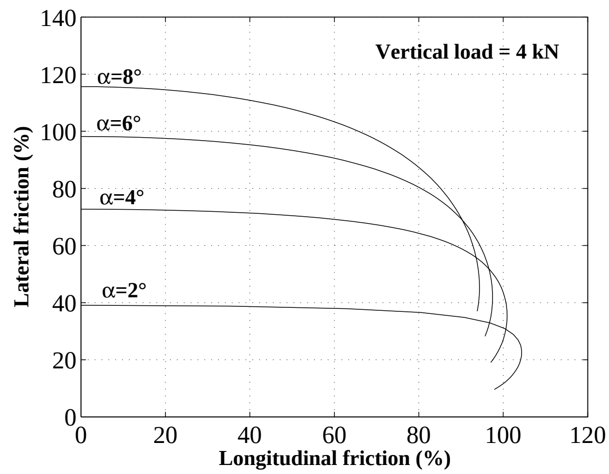

Fig. 7. Front tyre friction ellipses considered in the 14 degrees of freedom model, with different values of lateral slip angle α, for a constant vertical load of 4 kN.

V. Simulation results

In order to show in a realistic way the effectiveness of the proposed control approach, simulations of different maneuvers are performed using a detailed nonlinear 14 degrees of freedom vehicle model. In particular, the model degrees of freedom correspond to the standard three chassis translations and yaw, pitch, and roll angles, the four wheel angular speeds and the four wheel vertical movements with respect to the chassis. Nonlinear characteristics obtained on the basis of measurements on the real vehicle have been employed to model the tyre, steer and suspension behaviour. The employed tyre model is described e.g. in [22] and it takes into account the interaction between longitudinal and lateral slip, as well as vertical tyre load and suspension motion, to compute the tyre longitudinal and lateral forces and self–aligning moment. An example of the related tyre friction ellipses is showed in Fig. 7, where the lateral friction coefficient is reported as a function of the exploited longitudinal friction (during traction) and of the tyre slip angle α. Unsymmetrical friction ellipses for traction–braking longitudinal forces is also considered. Fig. 6 shows a comparison between the yaw rate measured on the real vehicle and the one obtained in simulation with the considered model. As can be seen, the model adopted in simulation gives a good description of the vehicle dynamics as compared with real data. To test the robustness feature of the proposed control scheme, in the following maneuvers, either the nominal vehicle configuration or a vehicle with increased mass (+ 300 kg, with consequent inertial and geometrical parameter variations) have been considered. The parameters of the single track model (3) considered for the control design are as follow $v = 100\,\text{km/h}= 27.77\,\text{m/s}$, $m = 1715\,\text{kg}$, $J_z = 2700\,\text{kgm}^2$, $a = 1.07\,\text{m}$, $b = 1.47\,\text{m}$, $l_f = 1\,\text{m}$, $l_r = 1\,\text{m}$, $c_f = 95117\,\text{Nm/rad}$, $c_r = 97556\,\text{Nm/rad}$ while the parameters of the RAD model (2) considered in simulation are $K_A = 2500$ Nm/A and $\omega_A = 53.4$ rad/s.

In principle, a value for the control gain K_{SL} in (16) can be found according to (17), relying on the knowledge of a suitable value of the bound Λ. However, in order to find a less conservative value of the control gain, one can also tune this parameter relying on simulation results, by choosing K_{SL} sufficiently high in order to guarantee the convergence to the sliding manifold and good performances. We have done so, and the chosen value of the control gain is $K_{SL} = 8000$. The objective function for the feedforward controller has been chosen as

$$T_\delta^{\text{des}}(s) = \frac{56.7}{s+10}$$

The bandwidth of the feedforward component has been chosen in simulation in order to achieve satisfactory performances.

A. Constant speed steering pad

The aim of this maneuver is to evaluate the steady–state vehicle performances: the steering angle is slowly increased (i.e. $1°/\text{s}$ handwheel velocity) while the vehicle is moving at constant speed, until the vehicle lateral acceleration limit is reached and the vehicle becomes unstable or the constant speed value cannot be kept. The results of this test, performed with a full load vehicle (+300 kg), are shown in Fig. The reference steering diagram and the one obtained with

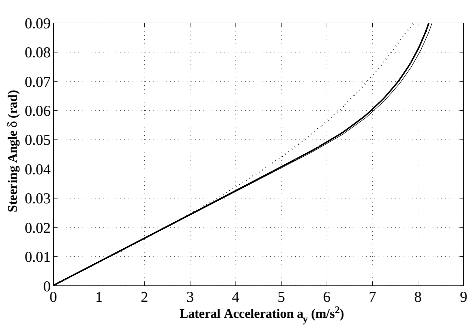

Fig. 8. Steering pad test at 100 km/h. Comparison between the reference steering diagram (thin solid line) and the ones obtained with the full load (+300 kg) uncontrolled vehicle (dotted) and with the controlled vehicle (solid).

the controlled vehicle are practically superimposed: thus the target vehicle behaviour, characterized by a lower understeer gradient, is reached by the proposed control system, which show good tracking performances also in the nonlinear tract

TABLE I
MAXIMUM AND RMS REFERENCE TRACKING ERRORS

Steering Pad	+300 kg	+200 kg	+100 kg	Nominal
E_{max}	$6.0 \cdot 10^{-4}$	$6.6 \cdot 10^{-4}$	$6.8 \cdot 10^{-4}$	$2.3 \cdot 10^{-4}$
E_{rms}	$4.0 \cdot 10^{-8}$	$4.2 \cdot 10^{-8}$	$4.9 \cdot 10^{-8}$	$2.8 \cdot 10^{-7}$
Steer Reversal	+300 kg	+200 kg	+100 kg	Nominal
E_{rms}	$3.5 \cdot 10^{-3}$	$2.1 \cdot 10^{-3}$	$1.8 \cdot 10^{-3}$	$1.8 \cdot 10^{-3}$

of the diagram and with changed vehicle characteristics. A small tracking error can be noted in the nonlinear zone at quite high lateral acceleration values. This is due to the fact that the car does not reach the steady state conditions (i.e. $a_y(t) \neq \dot{\psi}(t)v(t)$) because of its increased inertial characteristics. Fig. 9 shows the course of the tracking error $(\dot{\psi}_{\text{ref}} - \dot{\psi})$ in the initial part of the maneuver: it can be noted that a chattering phenomenon occurs. The chattering effect is due to the fact that the presence of the unmodelled RAD actuator increases the relative degree of the system. As a consequence, the transient process converge to a periodic motion [27], [28]. However, in the considered case the oscillations are too small to be perceived by the driver. A possible way to reduce the chattering is the use of lower values of the gain K_{SL} in the computation of the auxiliary control (16): however, the lower K_{SL} the worse the performance and robustness properties of the second order sliding mode controller [24]. Thus, a compromise has to be reached between limited chattering and good performances. The results of a more complete analysis of

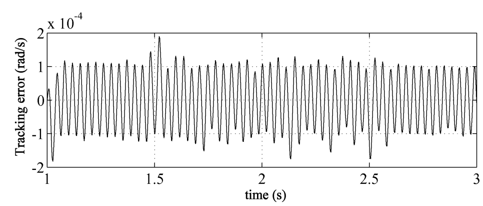

Fig. 9. Steering pad test at 100 km/h, full load (+300kg) conditions. Tracking error during the initial part of the test for the control system with nominal vehicle configurations.

the tracking performances obtained with the considered control strategies, for the steering pad maneuver, are reported in Table I, in terms of maximum error $E_{\text{max}} = \max_{t\in[t_0,t_{\text{end}}]} |\dot{\psi}_{\text{ref}}(t) - \dot{\psi}(t)|$ and root mean square error E_{rms}, i.e.,

$$E_{\text{rms}} = \sqrt{\frac{1}{t_{\text{end}} - t_0} \int_{t_0}^{t_{\text{end}}} (\dot{\psi}_{\text{ref}}(t) - \dot{\psi}(t))^2 dt} \tag{22}$$

where t_0 and t_{end} are the starting and final test time instants respectively. It can be noted that the proposed controller is able to achieve good tracking performance, with very low values of E_{rms} and E_{max}. Similar results have been obtained for different speed values.

B. Steer reversal test

This test aims at evaluating the controlled car transient response performances: in Fig. 10 the employed steering angle behaviour is showed, corresponding to a maximum handwheel angle of 50°, with a handwheel speed of 400°/s. The maneuver

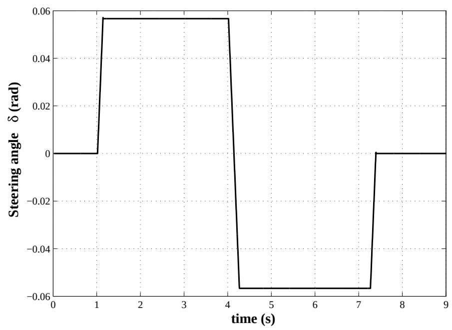

Fig. 10. Steering angle reversal test input corresponding to 50° handwheel angle

has been performed at 100 km/h. The obtained yaw rate course shows that the controlled vehicle dynamic response in nominal conditions is well damped (see Fig. 11). The time evolution of yaw moment M_z is reported in Fig. 12. Table I shows the tracking performance obtained in the 50° steer reversal maneuver with varying mass values, with consequent changes of the other inertial and geometrical parameters, in terms of root mean square error E_{rms}. It can be noted that the proposed SOSM controller achieves low values of E_{rms} also with increased mass, showing good robustness properties.

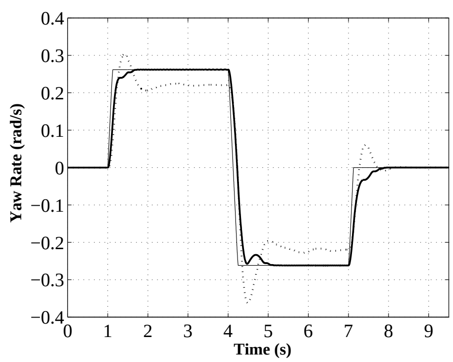

Fig. 11. 50° steer reversal test at 100 km/h, nominal conditions. Comparison between the reference yaw rate course (thin solid line) and the ones obtained with the uncontrolled (dotted) vehicle and the controlled (solid) vehicle.

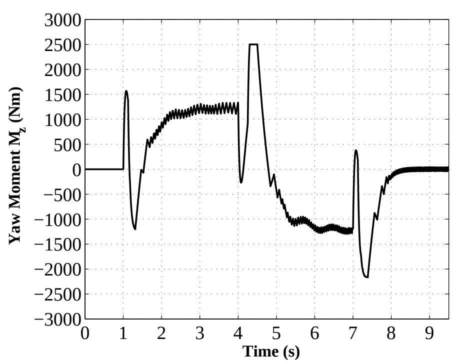

Fig. 12. 50° steer reversal test at 100 km/h, nominal conditions. Time evolution of the yaw moment.

C. ISO double lane change

The aim of this maneuver is to test the effectiveness of the proposed approach also in closed loop, i.e. in presence of the drivers' action. The ISO double lane change maneuver has been implemented as reported in [22], with constant test speed $v_{\text{ref}} = 100\,\text{km/h}$. The reference vehicle path in terms of yaw angle $\psi_{\text{ref}}(t)$ is reported in Fig. 13. The simple drivers' model described e.g. in [22] has been adopted:

$$\delta(s) = \frac{K_d}{\tau_d\, s + 1}\left(\psi_{\text{ref}}(s) - \psi(s)\right)$$

More complex driver models could be employed, however the purpose of the considered closed loop maneuver is to simply make a comparison between the handling properties of the uncontrolled vehicle and the controlled one, given the same driver model. The values of the driver gain K_d and of the driver time constant τ_d have been chosen as $K_d = 0.63$ and $\tau_d = 0.16\,\text{s}$. Note that the values of τ_d range approximately from $0.08\,\text{s}$ (experienced driver) to $0.25\,\text{s}$ (unexperienced driver), while the higher is the driver gain, the more aggressive is the driving action which could cause more likely vehicle instability. Fig. 14 shows the obtained results in terms of handwheel angle $\delta_H(t) = 15.4\,\delta(t)$: it can be noted that with the controlled vehicle the resulting driver input is less oscillating than the one obtained in the uncontrolled case, showing again that the considered control strategy achieves quite good improvements of the system damping properties.

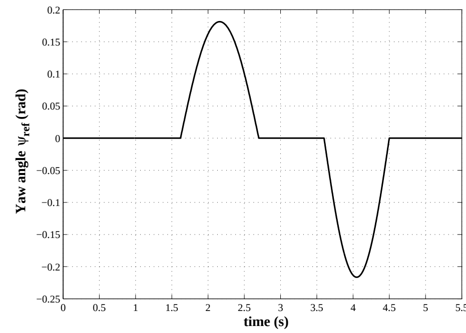

Fig. 13. Reference yaw angle $\psi_{\text{ref}}(t)$ for the ISO double lane change test at 100 km/h

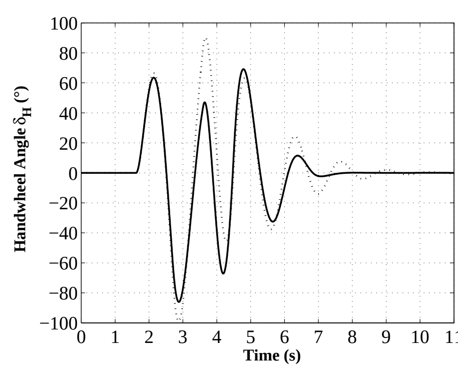

Fig. 14. ISO double lane change at 100 km/h, handwheel input δ_H for the full load (+300 kg) uncontrolled vehicle (dotted) and the controlled vehicle (solid).

VI. Conclusions

The problem of vehicle yaw control using yaw rate feedback and a Rear Active Differential has been investigated. The proposed control structure is composed by a reference generator, designed to improve vehicle handling, a feedforward contribution, which enhances the transient system response, and a feedback controller. The feedback controller is designed relying on the so–called second order sliding mode methodology which is capable of guaranteeing robust system stability in presence of disturbances and model uncertainties which are typical of the automotive context. Indeed, the proposed second order sliding mode controller generates a continuous control action, which is a particularly appropriate feature for applications in the automotive field, since it enables to limit the generation of vibrations which can propagate throughout the vehicle subsystems. The control scheme has been verified in simulation relying on an accurate 14 d.o.f. vehicle model. The obtained results show the effectiveness of the proposed control scheme. Quite good tracking performances have been obtained in steering pad maneuvers and good transient performances have been achieved in steer reversal tests and in lane change maneuvers. Simulation evidence has also assessed the robustness of the proposed controller, since the considered maneuvers have been performed with varying vehicle speed and mass.

References

[1] R. Rajamani, *Vehicle Dynamics and Control*, Springer–Verlag, New York, 2005.

[2] J. Ackermann and W. Sienel, “Robust yaw damping of cars with front and rear wheel steering," *IEEE Trans. on Control Systems Technology*, vol. 1, no. 1, pp. 15–20, 1993.

[3] J. Ackermann, J. Guldner, R. Steinhausner and V. I. Utkin, “Linear and nonlinear design for robust automatic steering," *IEEE Trans. on Control System Technology*, vol. 3, no. 1, pp. 132–143, 1995.

[4] B. A. Güvenç, T. Bünte and L. Güvenç, “Robust two degree-of-freedom vehicle steering controller design," *IEEE Trans. on Control System Technology*, vol. 12, no. 4, pp. 627–636, 2004.

[5] M. Canale, L. Fagiano, M. Milanese and P. Borodani, “Robust vehicle yaw control using an active differential and IMC techniques," *Control Engineering Practice*, no. 15, pp. 923–941, 2007

[6] M. Canale and L. Fagiano, “A robust imc approach for stability control of 4ws vehicles," *Vehicle Systems Dynamics, In print*, 2008.

[7] R. Daily and D.M. Bevly, “The use of GPS for vehicle stability control systems," *IEEE Trans. on Industrial Electronics*, Vol. 51, no. 2, pp. 270–277, 2004.

[8] J. Stephant, A. Charara, and D. Meizel, “Virtual sensor: application to vehicle sideslip angle and transversal forces," *IEEE Trans. on Industrial Electronics*, Vol. 51, no. 2, pp. 278–289, 2004.

[9] L. Ippolito, G. Lupo and A. Lorenzini “System for controlling torque distribution motor vehicle differential," *Patent no. US 2002/0016661 A1*, Applicant Centro Ricerche Fiat, 1992.

[10] S. Frediani, R. Gianoglio and F. Giuliano “System for the active control of a motor vehicle differential," *Patent no. US 2002/0016661 A1*, Applicant Centro Ricerche Fiat, 2002.

[11] D. Colombo, “Active Differential technology for yaw moment control," *6^{th} All wheel drive congress*, Graz , February 2005.

[12] M. Canale, L. Fagiano, A. Ferrara and C. Vecchio, “A Comparison Between IMC and Sliding Mode Approaches to Vehicle Yaw Control," *Proc. American Control Conference*, Seattle, WA, USA, 2008.

[13] M. Canale, L. Fagiano, A. Ferrara and C. Vecchio, “Comparing Internal Model Control and Sliding Mode Approaches for Vehicle Yaw Control," *IEEE Trans. on Intelligent Transportation Systems*, to appear.

[14] R. Avenati, S. Campo and L. Ippolito, “A rear active differential: theory and practice of a new type of controlled splitting differential and its impact on vehicle behaviour," *Global Powertrain Conference*, Detroit, October 1998.

[15] G. Bartolini, A. Ferrara, F. Levant and E. Usai, “On second order sliding mode controllers," in *Variable Structure Systems, Sliding Mode and Nonlinear Control*, K–K. David Young and Ü. Özgüner Eds. Lecture Notes in Control and Information Sciences, Springer–Verlag, vol. 247, pp. 329–350, 1999.

[16] A. Levant, “Sliding order and sliding accuracy in sliding mode control," *International Journal of Control*, vol. 58, pp. 1247–1263, 1993.

[17] G. Bartolini, A. Ferrara and E. Usai, “Chattering avoidance by second–order sliding mode control," *IEEE Trans. on Automatic Control*, Vol. 43, no. 2, pp. 241–246, 1998.

[18] G. Bartolini, A. Pisano, E. Punta, and E. Usai, “A survey of applications of second-order sliding mode control to mechanical systems," *International Journal of Control*, vol. 76, no. 9, pp. 875–892, 2003.

[19] V.I. Utkin, *Sliding Modes in Control and Optimization*, Springer–Verlag, New York, 1992.

[20] C. Edwards and K. S. Spurgeon, *Sliding mode control: theory and applications*, Taylor & Francis, London, U.K., 1998.

[21] S. Data and F. Frigerio, “Objective evaluation of handling quality," *Journal of Automobile Engineering*, vol. 216, no. 4 pp. 297–305, 2002.

[22] Genta, G., *Motor Vehicle Dynamics: Modeling and Simulation, II ed.*, World Scientific, Singapore, 2003.

[23] E. Bakker, L. Lidner and H.B. Pacejka, “A New Tyre Model with an Application in Vehicle Dynamics Studies," *SAE Paper 890087*, 1989.

[24] G. Bartolini, A. Ferrara and E. Usai, “Output tracking control of uncertain nonlinear second-order systems," *Automatica*, vol. 33, no. 12, pp.2203–2212, 1997.

[25] A. F. Filippov, *Differential Equations with Discontinuous Right–Hand Side*, Kluwer, Dordrecht, the Netherlands, 1988.

[26] A. Ferrara and M. Rubagotti, “A sub–optimal second order sliding mode controller for systems with saturating actuators," *Proc. American Control Conference*, Seattle, WA, USA, 2008.

[27] I. Boiko, L. Fridman, A. Pisano and E. Usai, “Analysis of chattering in systems with second-order sliding modes," *IEEE Trans. on Automatic Control*, vol. 52, no. 11, pp. 2085–2102, 2007.

[28] I. Boiko, L. Fridman, A. Pisano and E. Usai, “Performance analysis of second-order sliding-mode control systems with fast actuators," *IEEE Trans. on Automatic Control*, vol. 52, no. 6, pp. 1053–1059, 2007.